No. 15

KEK 82- 7
September 1982
A

SIMULATION OF DEUTERON ACCELERATION IN THE KEK 20-MeV LINAC

Takao KATO

NATIONAL LABORATORY FOR
HIGH ENERGY PHYSICS

KEK Reports are available from

Technical Information Office
National Laboratory for High Energy Physics
Oho-machi, Tsukuba-gun
Ibaraki-ken, 305
JAPAN

Phone: 0298-64-1171
Telex: 3652-534 (Domestic)
(0)3652-534 (International)
Cable: KEKOHO

SIMULATION OF DEUTERON ACCELERATION IN THE KEK 20-MeV LINAC

Takao KATO

National Laboratory for High Energy Physics
Oho-machi, Tsukuba-gun, Ibaraki-ken, 305, Japan

Abstract

Simulation of deuteron acceleration in the KEK 20-MeV proton linac was performed. The acceleration with an injection energy of 555 keV instead of 375 keV is very promising. This option allows the same accelerating field distribution and the same focusing field strength as those for protons, though it requires the increase of rf power by 20 – 50 %. The longitudinal phase acceptance reaches 180° without a buncher if the energy spread of the injection particles is within ± 3 keV. Normarized transverse acceptance is found to be 1.45 πcm·mrad.

1. Introduction

Accerelation of deuterons in the KEK 20-MeV proton linac was discussed[1] several years ago where computer calculation of both the longitudinal and the transverse motions was carried out on the basis of the transit time factors of deuterons measured by a bead perturbation method[2]. They concluded that it would be rather easy to accelerate deuterons with an injection energy nearly equal to half the proton injection energy if the optimum field distribution could be obtaind by careful tuning of fourteen movable frequency tuners of the tank.

In acceleration of deuterons in an Alvarez proton linac, it is required to satisfy the synchronous condition limited by the existing tank structures. Provided that deuterons travel on the same stable rf phase angle as protons, there are two modes of acceleration. One is the 2π-mode which is already employed for protons. In this mode the velocity of deuteron should be the same as that of proton and thus the output energy of deuteron is twice as large as that of proton. It also requires to double the injection energy, the accelerating field strength and the focusing field strength, which seem to be inappropriate values to our machine facilities.

The other is the 4π-mode in which deuterons travel one cell during two rf periods. In this mode the injection energy of deuterons should be half the energy of protons, while the momenta of both particles are equal and the focusing field strength should be also equal. This mode was demonstrated at the BNL 10-MeV linac[3] and was employed in the 20-MeV Saturne linac to accelerate deuterons, helium[4] and polarized protons[5].

From the synchronous conditions for protons and deuterons, the following relation is derived for each cell in non-relativistic limit,

$$E_p T_p L \cos\psi_p = 2 E_d T_d L \cos\psi_d \quad , \qquad (1)$$

where E_p = accelerating field for proton,

E_d = accelerating field for deuteron,

T_p = transit time factor of proton,

T_d = transit time factor of deuteron,

L = cell length,

ψ_p = stable phase angle for proton,

ψ_d = stable phase angle for deuteron.

We found from the relation (1) that if the ratio of T_p to T_d keeps constant throughout the tank, there is no need to change the accelerating field distribution along the tank. In particular when $T_p = 2T_d$, the accelerating field strength for both particles is exactly the same.

Fig. 1 shows the measured transit time factors for protons (T_p) and for deuterons (T_d) in the KEK 20-MeV linac[2]. Unfortunately the ratio of T_p to T_d varies greatly along the tank. Fig. 2 shows the designed accelerating field (E_p) for protons and the optimum accelerating field (E_d) for deuterons calculated by the relation (1). In our tank the designed accelerating field distribution is tilted as

$$E = 1.5 + 0.04z \ (\mathrm{Mv/m}) \quad , \qquad (2)$$

where z is the length in m measured from the low energy end. The injection energy of proton is assumed to be 750 keV and the output one 20.8 MeV. For deuteron acceleration in the optimum field distribution shown in Fig. 2, it is necessary to make a large change in the existing field distribution, which might be done by tuning the fourteen frequency tuners.

S. Ohnuma and Th. Sluyters pointed out in their study of deuteron acceleration that there is another promising injection energy which is much higher than half the proton injection energy[3]. According to their preliminary results, a large longitudinal acceptance (150°) would be expected with an injection energy of 545 keV, provided the energy spread of the injection particles is kept within 1 keV.

Since we do not have sufficient knowledge of getting the desired field distribution by the use of tuners, it is desirable to find the conditions of acceleration of deuterons which can be attained with a minimum change of tuners. Under such a field distribution, alternating acceleration of protons and deuterons is possible with a negligible time of tuning.

2. Calculation

Computer calculation was performed using modified PARMILA code in which some modifications were added to accelerate deuterons in a proton linac. The transit time factors used in the calculation are based on ref. (2) and shown in Fig. 1.

We assume eight types of accelerating field distribution for

acceleration of deuterons,

type-1) the optimum field,

type-2) the proton field,

type-3) the proton field multiplied by a factor of 1.1,

type-4) the proton field multiplied by a factor of 1.2,

type-5) the proton field multiplied by a factor of 1.3,

type-6) a constant field of 1.8 MV/m,

type-7) a constant field of 2.0 MV/m,

type-8) a constant field of 2.2 MV/m,

where the proton field means the designed field distribution for protons represented by eq. (2).

2.1 Longitudinal motion

To find a longitudinal acceptance, we start with the test particles shown in Fig. 3. From Fig. 4 to Fig. 11 we show the transmitted particles in an input phase space. The remarkable feature is the existence of the continuous passband in addition to a well known "golf-club" acceptance. In the optimum field distribution, we obtain a longitudinal acceptance like a golf-club located at the center energy of 375 keV shown in Fig. 12. The output emittance is shown in Fig. 13. There are not transmitted particles in a constant field below 1.6 MV/m.

The details of the "stomach-like" passband around the injection energy of 555 keV were studied. The results are shown in Fig. 14 – Fig. 27. In the proton field with an injection energy of 553 keV, we have

the phase acceptance of 60° (Fig. 14) if the energy spread of input particles is within % 1 keV. The longitudinal acceptance increases with the increase of the strength of the accelerating field and reaches 180° in the type-5 field with the energy acceptance of ± 3 keV (Fig. 20).

Longitudinal phase oscillations versus cell numbers are represented in Fig. 28 – Fig. 36. It is found that the deuteron with an injection energy of 555 keV travels in the low energy part of the tank as if it moves in a buncher. The amplitudes of phase oscillations are larger than those in the optimum field with an injection energy of 375 keV, leading to a large distribution of the output emitances in the eight types of accelerating field.

Fig. 37 shows the longitudinal capture efficiency of deuterons for eight field distributions. It seems very attractive to use these injection energy regions in acceleration of deuterons. In this case we need not change the field distribution, though some extra rf power is required to raise the accelerating field strength. This increase of an rf power (20 – 50 %) is quite easy since a big power of 2 MW for beam loading compensation in the usual acceleration of high intensity proton beam would be used to increase the accelerating field strength in the acceleration of low intensity deuteron beam. Choosing the injection energy of this region, we can not expect a large increase of capture efficiency by using a buncher because the energy acceptance is more or less a few keV. However, capture efficiency of more than 40 % will be expected without a buncher.

One disadvantage in the selection of higher injection energy is to increase the focusing strength in the beam transport line between the preaccelerator and the linac. The required increase of focusing strength

is 21 % and 33 % for the inejction energy of 555 keV and 660 keV respectively. If the focusing strength could be increased by 33 %, the higher passband around the injection energy of 660 keV is also promising. In this case we could expect more increase of beam intensity in the ion source since a current density is proportional to $V^{3/2}$, where V is a voltage of the extraction electrode and is equal to the injection energy.

2.2 Transverse motion

Transverse motions were calculated under the designed focusing field strength for protons[6] which has a magnetic field gradient of 110 Wb/m^3 at the tank entrance.

The input acceptance and the output emittance are shown in Fig. 38 – Fig. 53 for eight accelerating field distributions. The normarized acceptance of 1.47 πcm·mrad is obtained in the optimum field with an injection energy of 375 keV. In other cases with higher injection energy almost the same acceptances as in the optimum field are obtained. From the results of calculation, it is not necessary to change the focusing strength in the low energy part of the tank. There is no problem in the tranverse motion since a normalized emittance of 0.5 !cm"mrad is easily obtained at the injection end of the linac by the duoplasmatron ion source used in KEK[7].

Summary of the acceleration of deuterons is shown in Table 1. The output energy spread is within ± 100 keV except for the cases of type-6 and type-7.

3. Conclusion

Detailed computer calculation was performed to study the conditions of the acceleration of deuterons in the KEK 20-MeV linac. It is found that the acceleration with an injection energy of 555 keV instead of 375 keV is very promising. There is no need to change the accelerating field distribution and the focusing field strength which are employed for protons, though the increase of rf input power by 20 – 50 % is needed. The longitudinal phase acceptance reaches 180° without a buncher if the energy spread of the injection particles is within ± 3 keV. Normarized transverse acceptance is found to be about 1.45 πcm·mrad.

Acknowledgements

The author would like to express his sincere thanks to Prof. S. Fukumoto for recommendation of this work and valuable discussions and to Prof. E. Takasaki for many discussions on the computational problem. He wishes to thank Dr. D.A. Swenson for introducing the computer code of PARMILA from Los Alamos Scientific Laboratory.

References

1) M. Kobayashi, Y. Mizumachi and S. Okumura: KEK report, KEK-75-8 (1975).

2) S. Okumura and D.A. Swenson: KEK report, KEK-74-15 (1975).

3) S. Ohnuma and Th. Sluyters: Proc. 1972 Linac Conf., Los Alamos, 1972, p. 191.

4) JP. Auclair, PA. Chamouard and JL. Lemaire: Proc. 1979 Linac Conf., Montauk, 1979, p.37.

5) PA. Chamouard, JM. Lagniel and JL. Lemaire: Proc. 1981 Linac Conf., Los Alamos, 1981, p. 352.

6) M. Kobayashi: KEK report, KEK-73-4 (1973).

7) S. Fukumoto: private communication.

Table 1 Summary of acceleration of deuterons

Type of accelerating field	Injection energy (keV)	Capture efficiency (%)	Output energy spread (keV)	Normarized acceptance (πcm·mrad)	Required rf power (MW)
1. Optimum field	375	18	57	1.47	0.91
Optimum field with a buncher	375	65	157	1.47	0.91
2. Proton field	553	17	190	1.45	0.97
3. Proton field x 1.1	553	33	157	1.45	1.17
4. Proton field x 1.2	555	40	195	1.40	1.40
5. Proton field x 1.3	555	50	175	1.40	1.64
6. 1.8 MV/m	555	39	272	1.45	0.95
7. 2.0 MV/m	555	50	282	1.40	1.16
8. 2.2 MV/m	557	50	139	1.40	1.41

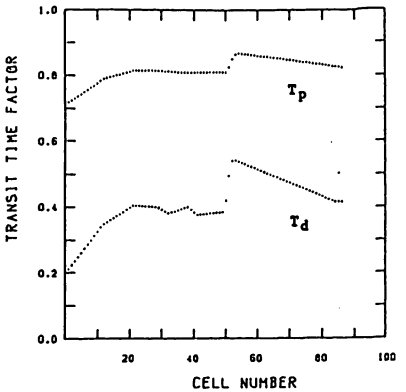

Fig. 1 Measured transit time factors for protons (T_p) and for deuterons (T_d) in the KEK 20-MeV linac.

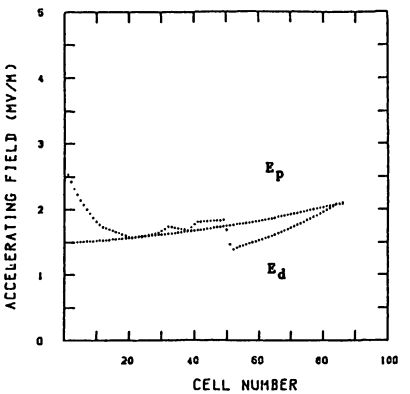

Fig. 2 Designed accelerating field for protons (E_p) and the optimum accelerating field for deuterons (E_d) calculated by eq. (1).

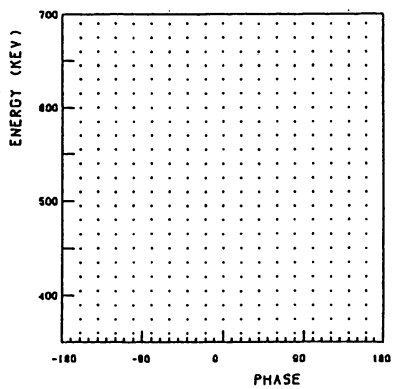

Fig. 3 Test particles in ψ - W phase space for finding a longitudinal acceptance. Energy is distributed from 360 keV to 690 keV in 15 keV step and phase -180° to 180° in 20° step.

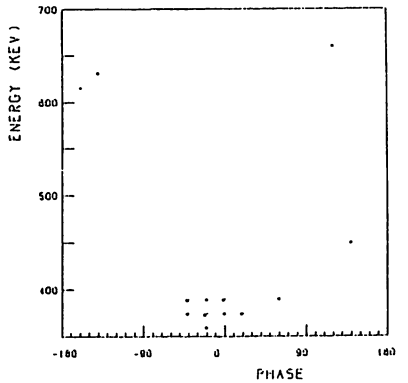

Fig. 4 Transmitted particles in the optimum field in an input phase space.

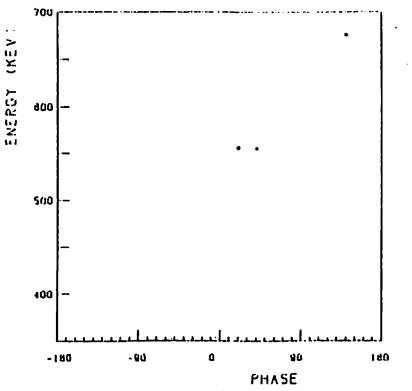

Fig. 5 Transmitted particles in the proton field in an input phase space.

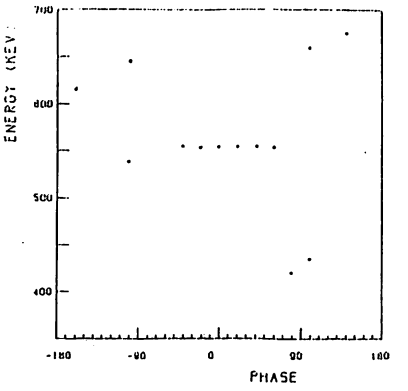

Fig. 6 Transmitted particles in the proton field x 1.1 in an input phase space.

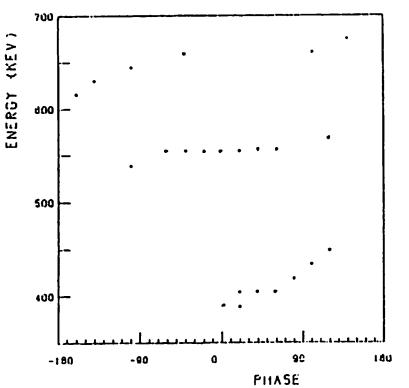

Fig. 7 Transmitted particles in the proton field x 1.2 in an input phase space.

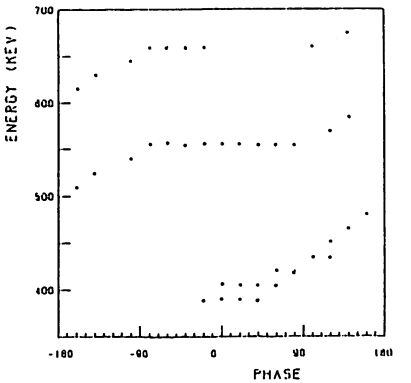

Fig. 8 Transmitted particles in the proton field x 1.3 in an input phase space.

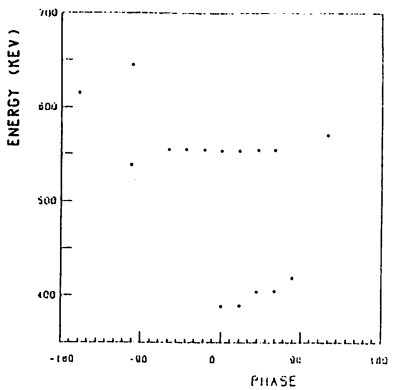

Fig. 9 Transmitted particles in the field of 1.8 MV/m in an input phase space.

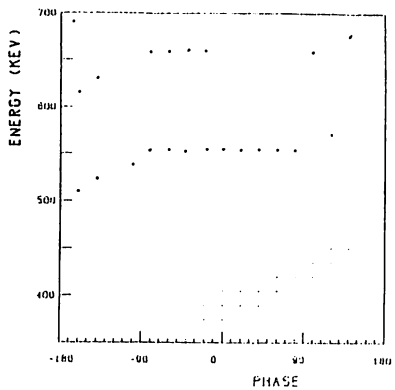

Fig. 10 Transmitted particles in the field of 2.0 MV/m in an input phase space.

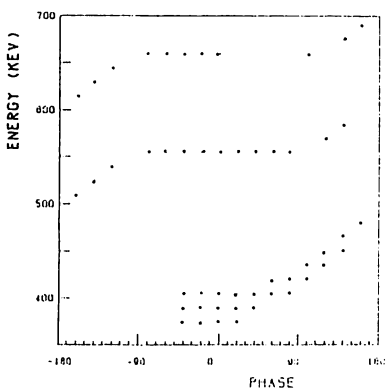

Fig. 11 Transmitted particles in the field of 2.2 MV/m in an input phase space.

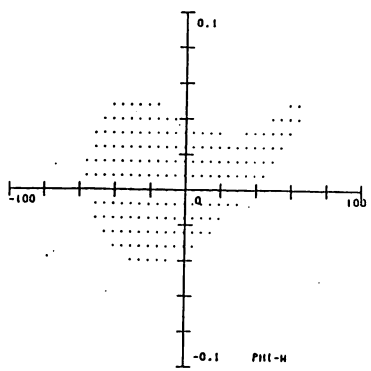

Fig. 12 Longitudinal acceptance in the optimum field.
Horizontal: 20° /div,
vertical: 7.5 keV/div.

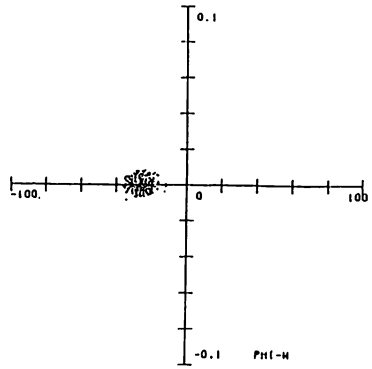

Fig. 13 Longitudinal output emittance in the optimum field.
Horizontal: 20° /div,
vertical: 200 keV/div.

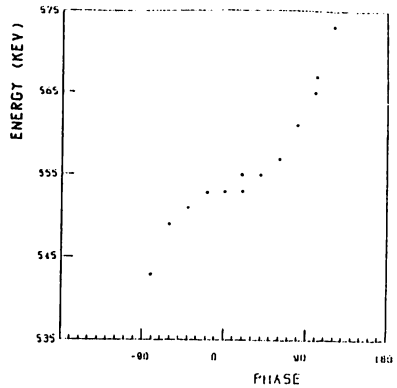

Fig. 14 Details of longitudinal acceptance in the proton field.

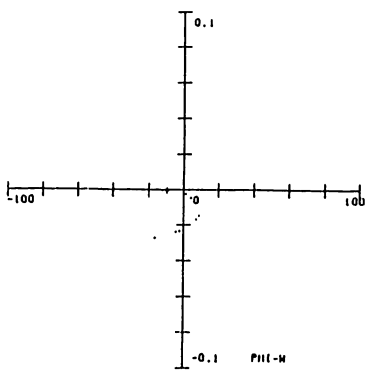

Fig. 15 Longitudinal output emittance in the proton field.
Horizontal: 20° /div,
vertical: 200 keV/div.

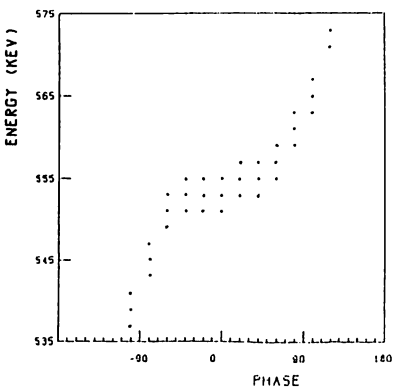

Fig. 16 Details of longitudinal acceptance in the proton field x 1.1.

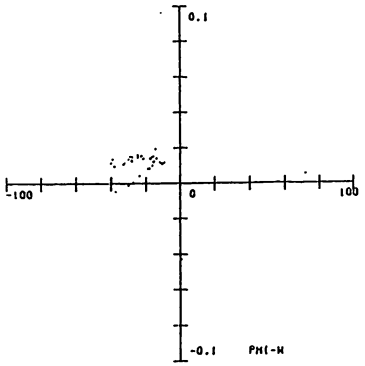

Fig. 17 Longitudinal output emittance in the proton field x 1.1.
Horizontal: 20° /div,
vertical: 200 keV/div.

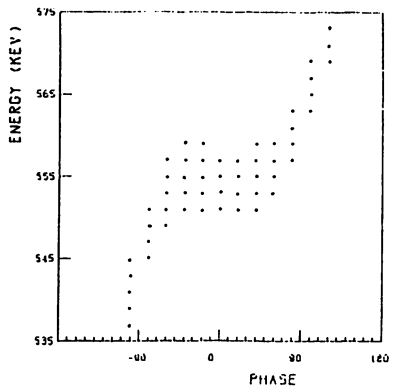

Fig. 18 Details of longitudinal acceptance in the proton field x 1.2.

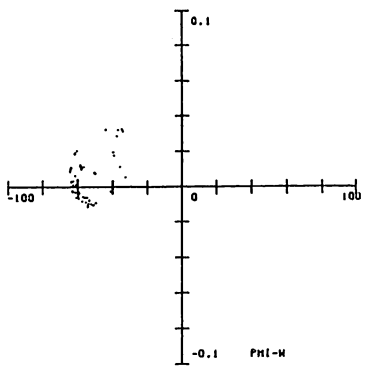

Fig. 19 Longitudinal output emittance in the proton field x 1.2.
Horizontal: 20° /div,
vettical: 200 keV/div.

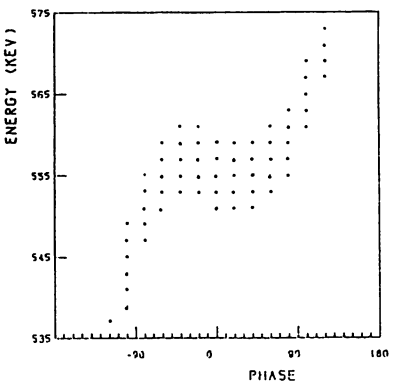

Fig. 20 Details of longitudinal acceptance in the proton field x 1.3.

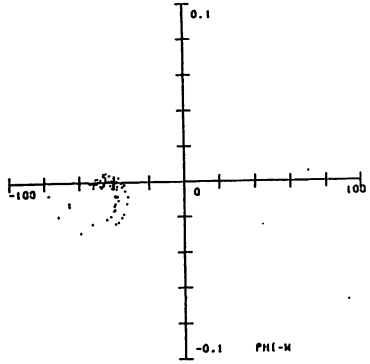

Fig. 21 Longitudinal output emittance in the proton field x 1.3.
Horizontal: 20° /div,
vertical: 200 keV/div.

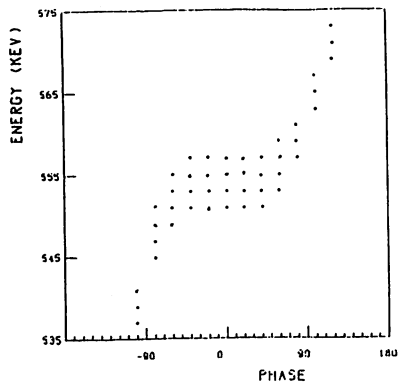

Fig. 22 Details of longitudinal acceptance in the field of 1.8 MV/m.

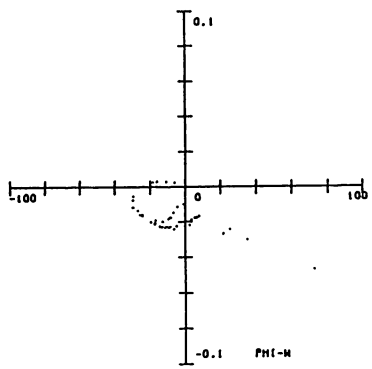

Fig. 23 Longitudinal output emittance in the field of 1.8 MV/m.
Horizontal: 20° /div,
vertical: 200 keV/div.

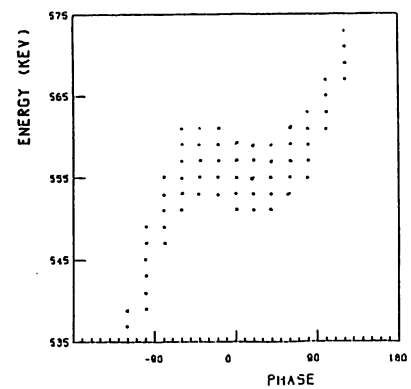

Fig. 24 Details of longitudinal acceptance in the field of 2.0 MV/m.
Horizontal: 20° /div,
vertical: 200 keV/div.

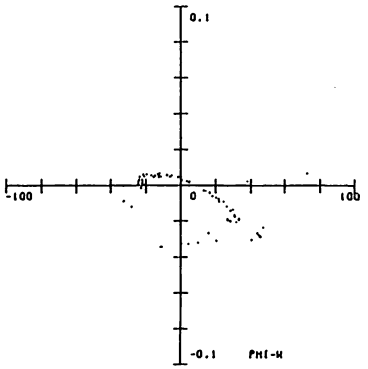

Fig. 25 Longitudinal output emittance in the field of 2.0 MV/m.
Horizontal: 20° /div,
vertical: 200 keV/div.

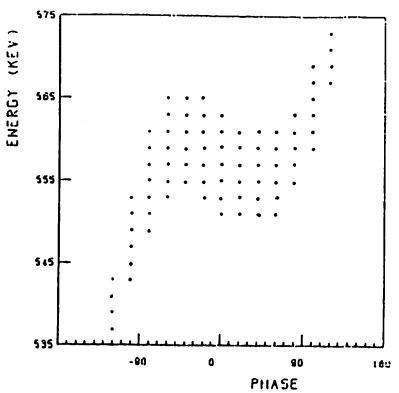

Fig. 26 Details of longitudinal acceptance in the field of 2.2 MV/m.

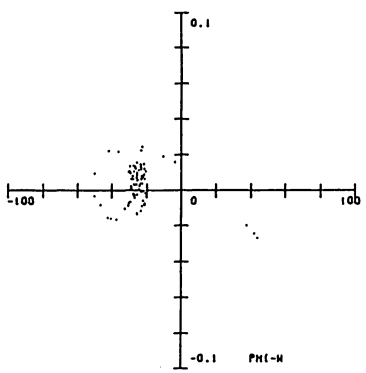

Fig. 27 Longitudinal output emittance in the field of 2.2 MV/m.
Horizontal: 20° /div,
vertical: 200 keV/div.

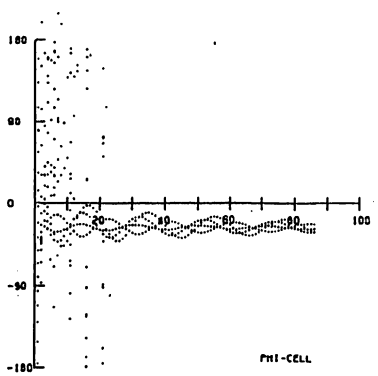

Fig. 28 Phase oscillations in the optimum field.
Injection energy W_{in} = 375 keV,
injection energy spread ΔW = 0.

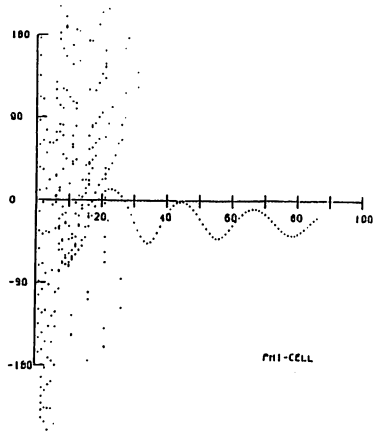

Fig. 29 Phase oscillation in the optimum field. W_{in} = 550 keV,
ΔW = 0.

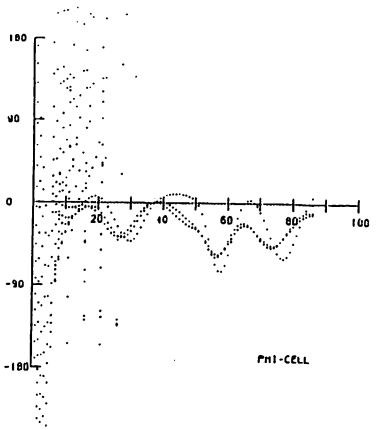

Fig. 30 Phase oscillations in the proton field. W_{in} = 553 keV,
ΔW = 0.

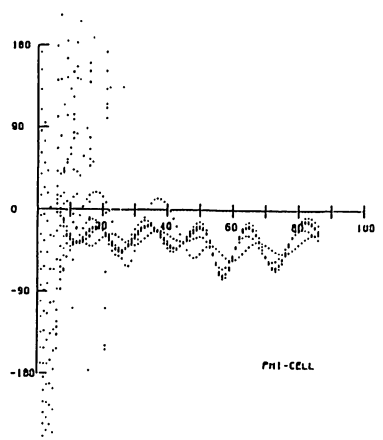

Fig. 31 Phase oscillations in the proton field x 1.1. W_{in} = 553 keV,
ΔW = 0.

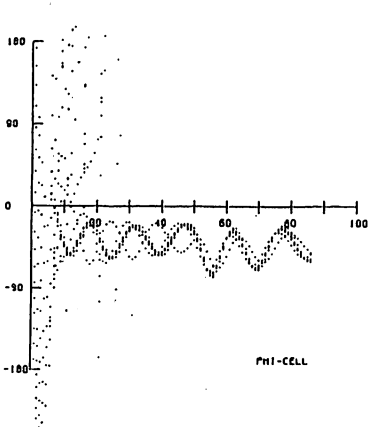

Fig. 32 Phase oscillations in the proton field x 1.2. W_{in} = 553 keV,
ΔW = 0.

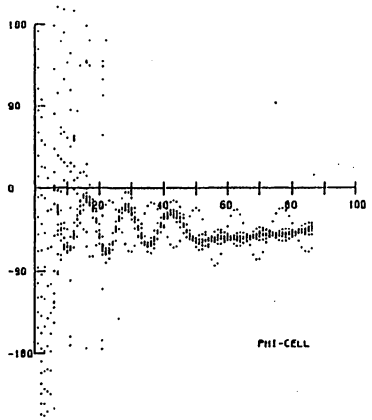

Fig. 33 Phase oscillations in the proton field x 1.3. W_{in} = 555 keV, ΔW = 0.

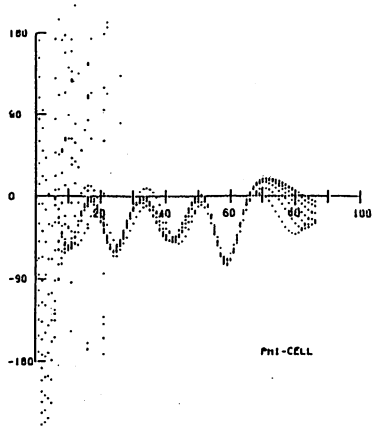

Fig. 34 Phase oscillation in the field of 1.8 MV/m. W_{in} = 555 keV, ΔW = 0.

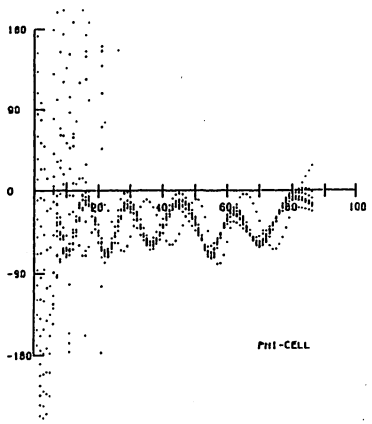

Fig. 35 Phase oscillations in the field of 2.0 MV/m. W_{in} = 555 keV, ΔW = 0.

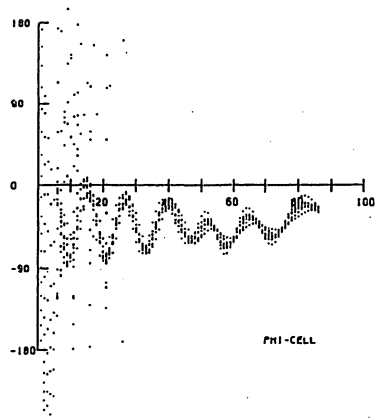

Fig. 36 Phase oscillations in the field of 2.2 MV/m. W_{in} = 557 keV, ΔW = 0.

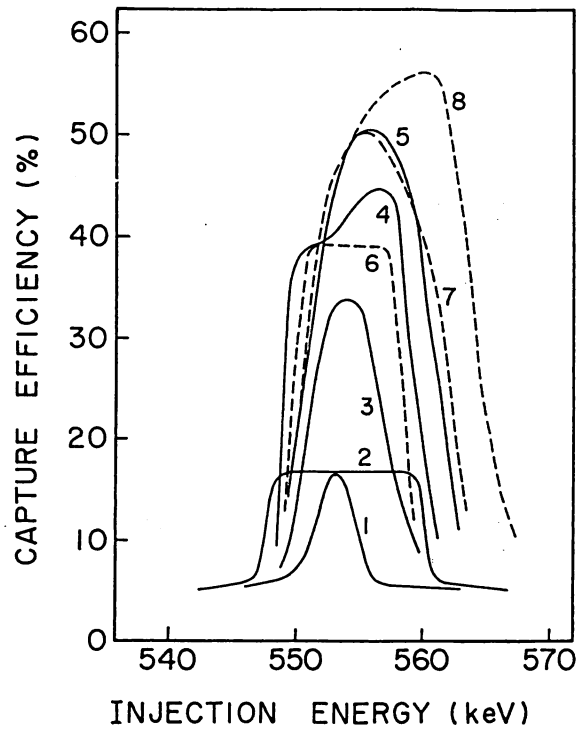

Fig. 37 Longitudinal capture efficiency for eight field distributions.

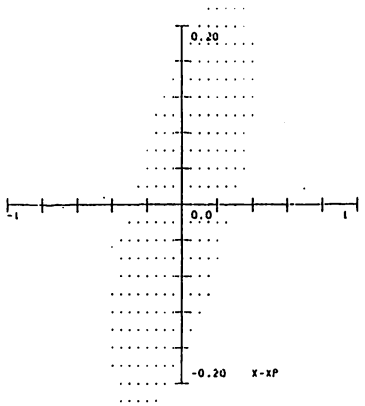

Fig. 38 Transverse input acceptance (x-x') in the optimum field.
Horizontal: 0.2 cm/div,
vertical: 0.04 rad/div.

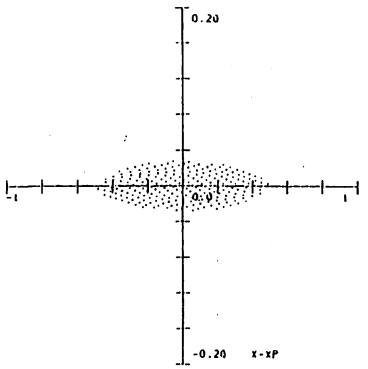

Fig. 39 Transverse output emittance (x-x') in the optimum field.
Horizontal: 0.2 cm/div,
vertical: 0.04 rad/div.

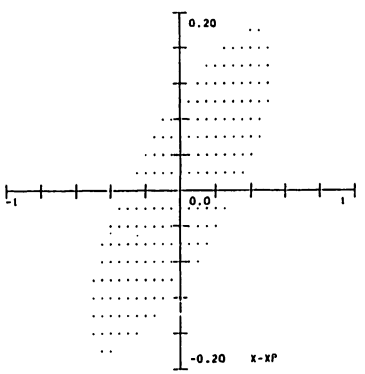

Fig. 40 Transverse input acceptance (x-x') in the proton field.
Horizontal: 0.2 cm/div,
vertical: 0.04 rad/div.

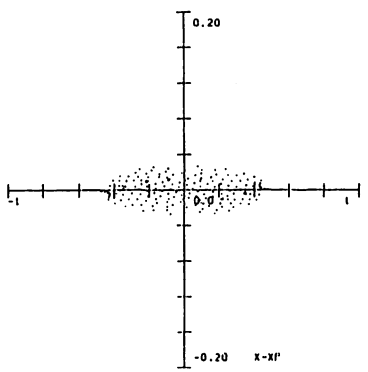

Fig. 41 Transverse output emittance (x-x') in the proton field.
Horizontal: 0.2 cm/div,
vertical: 0.04 rad/div.

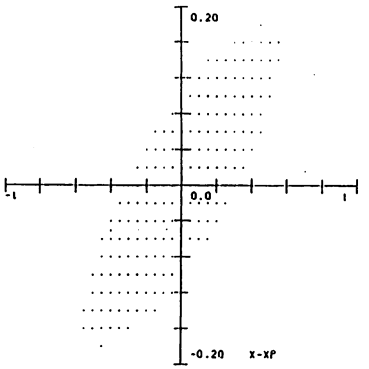

Fig. 42 Transverse input acceptance (x-x') in the proton field x 1.1.
Horizontal: 0.2 cm/div,
vertical: 0.04 rad/div.

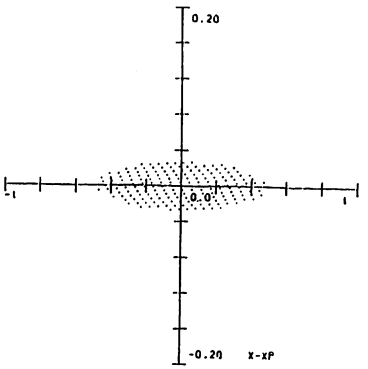

Fig. 43 Transverse output emittance (x-x') in the proton field x 1.1.
Horizontal: 0.2 cm/div,
vertical: 0.04 rad/div.

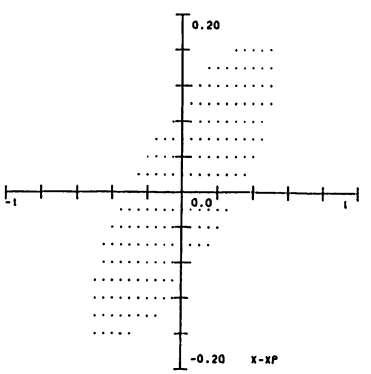

Fig. 44 Transverse input acceptance (x-x') in the proton field x 1.2.
Horizontal: 0.2 cm/div,
vertical: 0.04 rad/div.

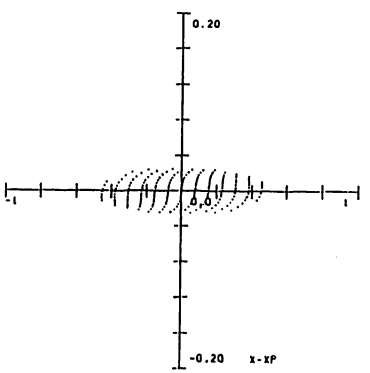

Fig. 45 Transverse output emittance (x-x') in the proton field x 1.2.
Horizontal: 0.2 cm/div,
vertical: 0.04 rad/div.

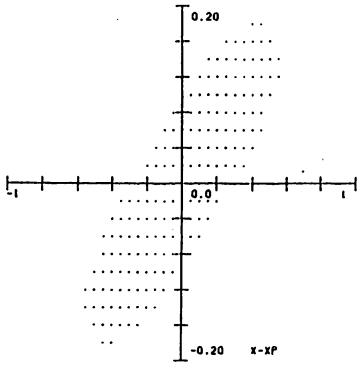

Fig. 46 Transverse input acceptance (x-x') in the proton field x 1.3.
Horizontal: 0.2 cm/div,
vertical: 0.04 rad/div.

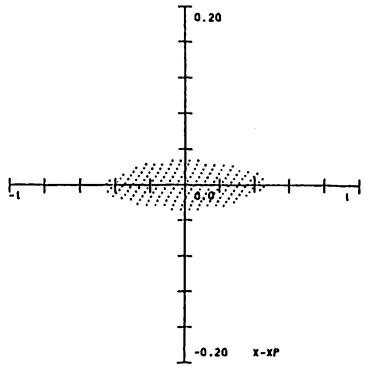

Fig. 47 Transverse output emittance (x-x') in the proton field x 1.3.
Horizontal: 0.2 cm/div,
vertical: 0.04 rad/div.

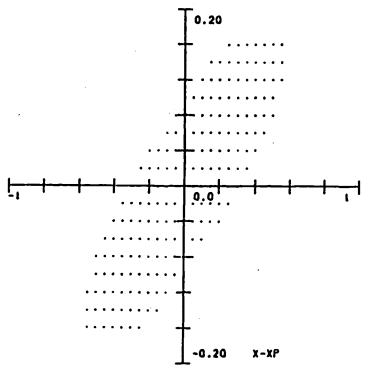

Fig. 48 Transverse input acceptance (x-x') in the constant field of 1.8 MV/m.
Horizontal: 0.2 cm/div,
vertical: 0.04 rad/div.

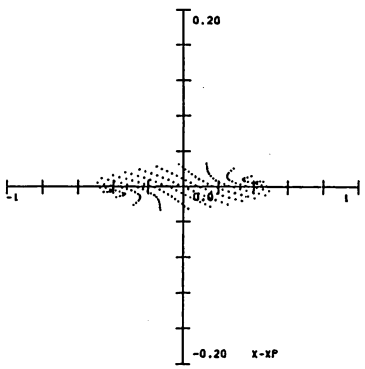

Fig. 49 Transverse output emittance (x-x') in the constant field of 1.8 MV/m.
Horizontal: 0.2 cm/div,
vertical: 0.04 rad/div.

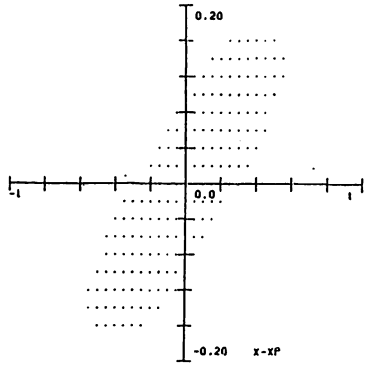

Fig. 50 Transverse input acceptance (x-x') in the constant field of 2.0 MV/m.
Horizontal: 0.2 cm/div,
vertical: 0.04 rad/div.

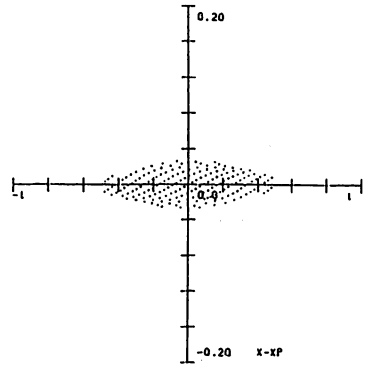

Fig. 51 Transverse output emittance (x-x') in the constant field of 2.0 MV/m.
Horizontal: 0.2 cm/div,
vertical: 0.04 rad/div.

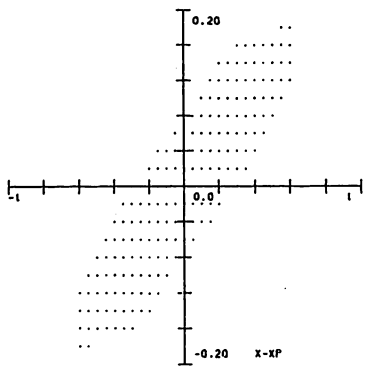

Fig. 52 Transverse input acceptance (x-x') in the constant field of 2.2 MV/m.
Horizontal: 0.2 cm/div,
vertical: 0.04 rad/div.

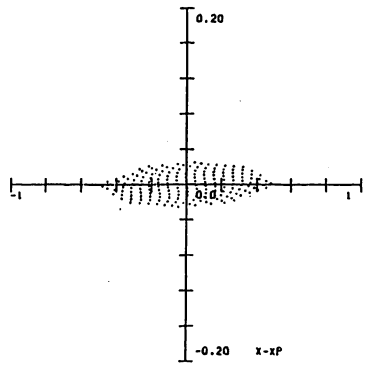

Fig. 53 Transverse output emittance (x-x') in the constant field of 2.2 MV/m.
Horizontal: 0.2 cm/div,
vertical: 0.04 rad/div.